

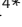
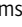
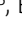




**BRIEF DEFINITIVE REPORT**

# Adaptive NK cells in people exposed to *Plasmodium falciparum* correlate with protection from malaria

Geoffrey T. Hart<sup>1,2</sup> , Tuan M. Tran<sup>3\*</sup> , Jakob Theorell<sup>4\*</sup> , Heinrich Schlums<sup>4</sup> , Gunjan Arora<sup>1</sup>, Sumati Rajagopalan<sup>1</sup>, A.D. Jules Sangala<sup>1,2</sup>, Kerry J. Welsh<sup>5</sup>, Boubacar Traore<sup>6</sup>, Susan K. Pierce<sup>1</sup> , Peter D. Crompton<sup>1</sup>, Yenan T. Bryceson<sup>4</sup> , and Eric O. Long<sup>1</sup> 

**How antibodies naturally acquired during *Plasmodium falciparum* infection provide clinical immunity to blood-stage malaria is unclear. We studied the function of natural killer (NK) cells in people living in a malaria-endemic region of Mali. Multi-parameter flow cytometry revealed a high proportion of adaptive NK cells, which are defined by the loss of transcription factor PLZF and Fc receptor  $\gamma$ -chain. Adaptive NK cells dominated antibody-dependent cellular cytotoxicity responses, and their frequency within total NK cells correlated with lower parasitemia and resistance to malaria. *P. falciparum*-infected RBCs induced NK cell degranulation after addition of plasma from malaria-resistant individuals. Malaria-susceptible subjects with the largest increase in PLZF-negative NK cells during the transmission season had improved odds of resistance during the subsequent season. Thus, antibody-dependent lysis of *P. falciparum*-infected RBCs by NK cells may be a mechanism of acquired immunity to malaria. Consideration of antibody-dependent NK cell responses to *P. falciparum* antigens is therefore warranted in the design of malaria vaccines.**

## Introduction

Natural sterile immunity to *Plasmodium falciparum* is rarely if ever acquired even after years of chronic exposure (Tran et al., 2013). If sterile immunity is not achieved in the liver, vaccine recipients remain fully susceptible to the disease caused by blood-stage malaria. In malaria-endemic areas, clinical immunity develops over years of repeated infections and manifests as reduced blood-stage parasite load (parasitemia) and control of inflammatory responses (Portugal et al., 2017b). Antibodies to malaria antigens, which are essential for protection (Cohen et al., 1961; Crompton et al., 2014), may neutralize *P. falciparum* merozoites (Rotman et al., 1998), activate complement-mediated lysis of merozoites (Boyle et al., 2015), or trigger immune responses through Fc receptors. Antibodies to *P. falciparum* antigens expressed on infected RBCs trigger phagocytosis by monocytes (Khusmith and Druilhe, 1983) and antibody-dependent cellular cytotoxicity (ADCC) by natural killer (NK) cells (Arora et al., 2018). The potential of NK cell-mediated ADCC to protect individuals against malaria has not been examined (Wolf et al., 2017). The aim of this study was to evaluate phenotypic and functional attributes of NK cells in people

naturally exposed to *P. falciparum* and examine whether any parameter correlated with protection against *P. falciparum* infection.

Human peripheral blood NK cells are divided into a larger subset of CD56<sup>dim</sup> cells and a smaller subset of CD56<sup>bright</sup> (CD56<sup>bri</sup>) cells that do not express Fc $\gamma$ RIIIa (CD16) and lack ADCC activity. Recently, so-called “adaptive” NK cells with enhanced ADCC activity were described in CMV-infected individuals (Sun et al., 2009; Lopez-Vergès et al., 2011; Lee et al., 2015; Schlums et al., 2015). Adaptive NK cells are broadly defined as CD56<sup>dim</sup> cells that have lost expression of transcription factor promyelocytic leukemia zinc finger (PLZF) and of the signaling Fc receptor  $\gamma$ -chain (FcR $\gamma$ ) through epigenetic changes (Tesi et al., 2016). PLZF<sup>-</sup> FcR $\gamma$ <sup>-</sup> NK cells that expand during CMV infection express NKG2C, an activating receptor that binds to HLA-E, including HLA-E loaded with CMV-derived peptides (Holmes and Bryceson, 2016; Hammer et al., 2018). Information about adaptive NK cells in other diseases is very limited.

A longitudinal cohort study of malaria immunity in children and young adults was started in 2011 in Kalifabougou, Mali,

<sup>1</sup>Laboratory of Immunogenetics, National Institute of Allergy and Infectious Diseases, National Institutes of Health, Rockville, MD; <sup>2</sup>Division of Infectious Disease and International Medicine, Department of Medicine, Center for Immunology, University of Minnesota, Minneapolis, MN; <sup>3</sup>Division of Infectious Diseases, Department of Medicine, Indiana University School of Medicine, Indianapolis, IN; <sup>4</sup>Center for Hematology and Regenerative Medicine, Department of Medicine Huddinge, Karolinska Institutet, Stockholm, Sweden; <sup>5</sup>Clinical Chemistry Division, Department of Laboratory Medicine, National Institutes of Health, Bethesda, MD; <sup>6</sup>Malaria Research and Training Center, Department of Epidemiology of Parasitic Diseases, International Center of Excellence in Research, University of Sciences, Techniques and Technologies of Bamako, Bamako, Mali.

\*T.M. Tran and J. Theorell contributed equally to this paper; Correspondence to Eric O. Long: [elong@nih.gov](mailto:elong@nih.gov); Geoffrey T. Hart: [hart0792@umn.edu](mailto:hart0792@umn.edu).

© 2019 Hart et al. This article is distributed under the terms of an Attribution–Noncommercial–Share Alike–No Mirror Sites license for the first six months after the publication date (see <http://www.rupress.org/terms/>). After six months it is available under a Creative Commons License (Attribution–Noncommercial–Share Alike 4.0 International license, as described at <https://creativecommons.org/licenses/by-nc-sa/4.0/>).

where rainy seasons with intense *P. falciparum* malaria transmission predictably alternate with dry seasons during which malaria rarely occurs (Dumbo et al., 2014). Within this cohort, we found that the relative abundance of PLZF<sup>-</sup> FcRγ<sup>-</sup> NK cells correlated with decreased parasitemia and prospectively predicted protection from malaria symptoms. These adaptive NK cells had enhanced cytokine production and cytotoxic activity in response to antibody-dependent activation. As NK cells of study subjects were activated by *P. falciparum*-infected RBCs in the presence of plasma from malaria-resistant individuals, these findings support a functional contribution of NK cells to protection from malaria through enhanced ADCC toward *P. falciparum*-infected RBCs.

## Results and discussion

### High frequency of PLZF<sup>-</sup> FcRγ<sup>-</sup> NK cells in a cohort of malaria-exposed individuals

Peripheral blood mononuclear cells (PBMCs) from 163 subjects 2–22 yr of age (Fig. 1 A and Fig. S1 A) were collected before and after the malaria transmission season, which occurred between June and December 2013 (Fig. 1 B). In addition, PBMCs were collected from susceptible subjects at their first clinical malaria episode and again 7 d after treatment with artemether and lumefantrine. Approximately half of the subjects suffered at least one malaria episode during the transmission season (Fig. 1 C). A multi-parameter flow cytometry analysis of all samples collected in May showed that CD56<sup>bri</sup> NK cells constituted ~10% of total NK cells (Fig. 1 D) with the expected CD57<sup>-</sup> NKG2A<sup>+</sup> phenotype (Fig. 1 E). CD56<sup>dim</sup> NK cells had a high proportion of PLZF<sup>-</sup> (~70%) and FcRγ<sup>-</sup> (~40%) cells (Fig. 1 F), reminiscent of adaptive NK cells observed during CMV infection (Schlums et al., 2015). An aggregate of primary flow data for all subjects showed that CD56<sup>bri</sup> NK cells had intermediate fluorescence signals for FcRγ and Eat-2 and brighter signals for CD2, NKG2A, and Syk (Fig. 1 G). In this population of subjects as a whole (but not necessarily for every subject), CD56<sup>dim</sup> NK cells were bimodal for every marker tested (Fig. 1 G). The complexity of phenotypic subsets was illustrated by t-distributed stochastic neighbor embedding (t-SNE) plots (Fig. 1 H).

A direct comparison with NK phenotypic subsets in PBMCs of 18 Swedish adults, which were included in our analysis of Mali samples, showed that the major subsets enriched in Malian subjects share a CD57<sup>+</sup> NKG2A<sup>-</sup> PLZF<sup>-</sup> FcRγ<sup>-</sup> phenotype (Fig. S1 B).

Most plasma samples from Malian subjects were positive for antibodies to EBV and CMV, consistent with early seroconversion to EBV and CMV in African children (Manicklal et al., 2013; Bates and Brantsaeter, 2016). Phenotypic subsets of NK cells in the 12 EBV<sup>-</sup> subjects did not differ significantly from EBV<sup>+</sup> subjects (Fig. S1, C and D). CMV infection, which has a major impact on the human immune system (Brodin et al., 2015) and drives expansion of adaptive NK cells (Schlums et al., 2015), is likely to have contributed to the expansion of FcRγ<sup>-</sup> NK cells in the Mali cohort. As expected (Lopez-Vergès et al., 2011; Schlums et al., 2015), the 10 CMV<sup>-</sup> subjects had a lower proportion of NKG2C<sup>+</sup> and higher proportion of NKG2A<sup>+</sup> NK cells (Fig. S1 E).

However, the CMV<sup>-</sup> subjects had a frequency of FcRγ<sup>-</sup> NK cells similar to that of CMV<sup>+</sup> subjects (Fig. S1 E), suggesting that FcRγ<sup>-</sup> NK cells increase also in response to other stimuli.

Adaptive FcRγ<sup>-</sup> NK cells during CMV infection are mostly CD57<sup>+</sup> NKG2C<sup>+</sup> (Lopez-Vergès et al., 2011; Foley et al., 2012). In Malian subjects, however, FcRγ<sup>-</sup> NK cells included a higher proportion of CD57<sup>-</sup> NKG2C<sup>-</sup> NK cells than CD57<sup>+</sup> NKG2C<sup>+</sup> NK cells (Fig. S1 F), suggesting a greater diversity of adaptive NK cells in the Mali cohort.

### Correlation of FcRγ<sup>-</sup> NK cells with parameters of malaria

Resistance to malaria disease was monitored in two ways. One was to compare individuals who did not experience clinical symptoms (resistant) to those who had at least one episode of febrile malaria (susceptible; Fig. 1 A). The other measured the time elapsed from the beginning of the malaria transmission season to the first episode of febrile malaria (Fig. 1 C). A higher frequency of FcRγ<sup>-</sup> NK cells was significantly associated with disease resistance (Fig. 2 A). It follows that conventional FcRγ<sup>+</sup> NK cells were associated with sensitivity to malaria. Analysis of all NK cell subsets with single, double, and triple combinations of six markers (CD2, CD57, NKG2C, NKG2A, FcRγ, and PLZF) showed that those most significantly associated with resistance were FcRγ<sup>-</sup> PLZF<sup>-</sup> and FcRγ<sup>-</sup> NK cells ( $P < 0.0024$ ; Fig. S2 A). Furthermore, subjects with the highest proportion of FcRγ<sup>-</sup> NK cells before the malaria season experienced a significantly longer delay until the first malaria episode (Fig. 2 B). Comparison of all subsets with single, double, and triple combinations of the same six phenotypic markers revealed that enrichment of CD57<sup>-</sup> FcRγ<sup>-</sup> PLZF<sup>-</sup> or total FcRγ<sup>-</sup> NK cells had the most significant association with delayed onset of malaria ( $P < 0.0029$ ; Fig. S2 B). Therefore, by two different criteria—resistance to malaria symptoms and delayed onset of disease—a higher frequency of FcRγ<sup>-</sup> NK cells in May correlated with protection from malaria symptoms during the ensuing transmission season.

Among susceptible subjects, parasite load during acute malaria was inversely correlated with frequency of FcRγ<sup>-</sup> and PLZF<sup>-</sup> NK cells (Fig. 2 C). Resistant subjects had a significantly higher frequency of FcRγ<sup>-</sup> and PLZF<sup>-</sup> NK cells than those with a high parasite load during malaria (Fig. 2 D). Among multiple combinations of phenotypic markers, the FcRγ<sup>-</sup> PLZF<sup>-</sup> double-negative and FcRγ<sup>-</sup> NK cells were the most significantly associated with resistance ( $P < 0.0001$ ; Fig. S2 C). Among all phenotypic markers tested, FcRγ<sup>-</sup> was the only one strongly associated with every measure of resistance: reduced parasite load, increased probability of remaining disease-free, and delayed disease onset during the transmission season.

An essential component to malaria disease resistance is antibodies to *P. falciparum* antigens (Bustamante et al., 2017). Chronic exposure to *P. falciparum* infection leads to the production of atypical memory B cells, which fail to generate functionally mature memory B cells and long-lived plasma cells (Portugal et al., 2017a). As it takes years of repeated infections to acquire antibodies that provide clinical immunity, age is significantly correlated with resistance to malaria symptoms (Crompton et al., 2014) and inversely correlated with parasite load, as observed in our cohort ( $P = 0.004$ ; Fig. S2 D). Increased

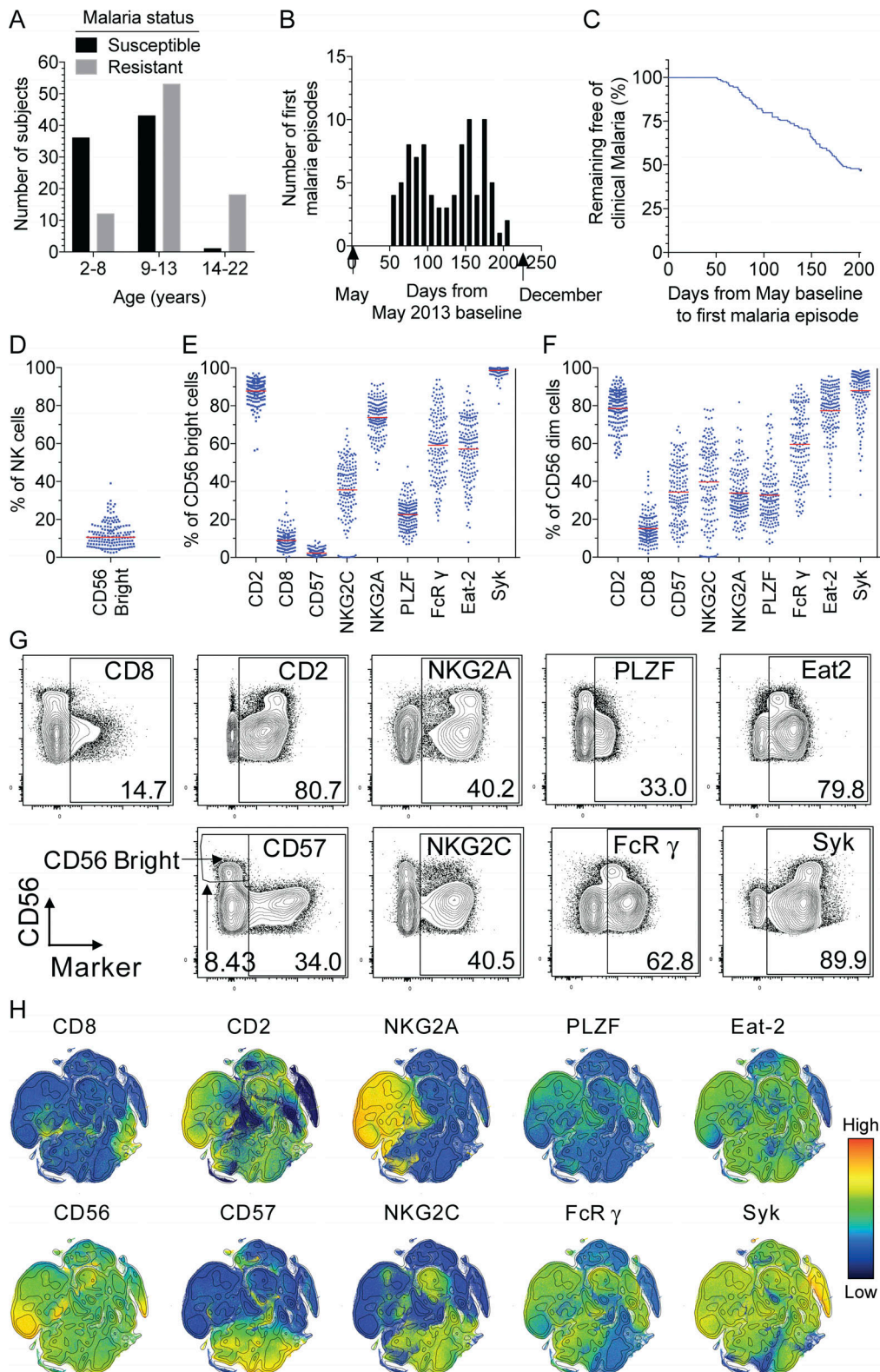


Figure 1. **NK cell phenotype of Malian subjects.** (A) Number of resistant and susceptible subjects in different age groups. (B) Incidence of malaria during the transmission season. (C) Probability of developing malaria symptoms during the transmission season. (D–F) Frequency of CD56<sup>bri</sup> NK cells among total NK cells (D) and of each indicated marker on CD56<sup>bri</sup> (E) and CD56<sup>dim</sup> (F) NK cells. Mean average is shown as a red bar. (G) Combined flow cytometry data files from all subjects at the May time point showing expression of phenotypic markers against CD56 expression. (H) t-SNE analysis of NK cell subsets for all subjects at the May time point. Expression of each marker is indicated by a color scale. Flow cytometry data in D–H was acquired over 15 independent experiments ( $n = 163$ ). Each experiment included internal controls described in the Materials and methods section.

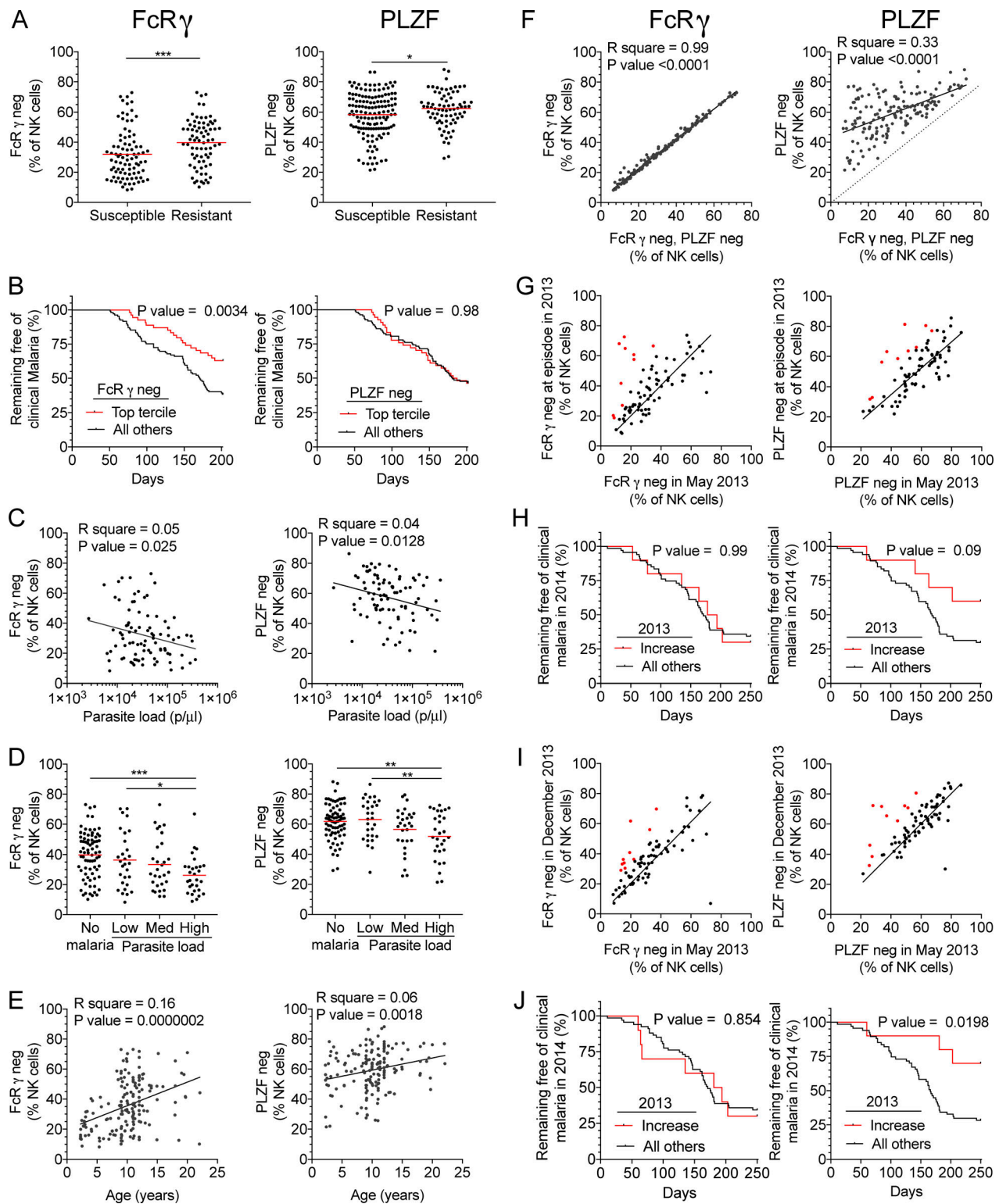


Figure 2. **Correlation of FcR $\gamma$ <sup>-</sup> and PLZF<sup>-</sup> NK cell frequency with protection against malaria.** (A) Frequency of FcR $\gamma$ <sup>-</sup> (left) and PLZF<sup>-</sup> (right) NK cells in susceptible and resistant subjects. Unpaired Student's *t* tests, \*\*\*, *P* < 0.001; \*, *P* < 0.05. (B) Time to first malaria episode in subjects separated into the top tercile with the highest frequency of FcR $\gamma$ <sup>-</sup> (left) or PLZF<sup>-</sup> (right) NK cells and all other subjects. *P* values determined with log rank Mantel-Cox test. (C) Frequency of FcR $\gamma$ <sup>-</sup> (left) and PLZF<sup>-</sup> (right) NK cells versus parasite density (parasites/ $\mu$ l) on a log scale. *R*<sup>2</sup> goodness-of-fit analysis on nonlinear regression line is shown. *P* values determined by Pearson correlation. *p*, parasites. (D) Frequency of FcR $\gamma$ <sup>-</sup> (left) and PLZF<sup>-</sup> (right) NK cells in resistant subjects (no malaria) compared with subjects ranked in terciles with low, medium (Med), or high parasite load. One-way ANOVA was done with post hoc test comparing low, medium, and high groups to the no malaria group only. \*\*\*, *P* < 0.001; \*\*, *P* < 0.01; \*, *P* < 0.05. (E) Frequency of FcR $\gamma$ <sup>-</sup> (left) and PLZF<sup>-</sup> (right) NK cells in subjects ranked by age. *R*<sup>2</sup> and *P* values determined as in C. (F) Frequency of FcR $\gamma$ <sup>-</sup> (left) and PLZF<sup>-</sup> (right) NK cells versus frequency of FcR $\gamma$ <sup>-</sup> PLZF<sup>-</sup> double-negative NK cells. *R*<sup>2</sup> and *P* values determined as in C. (G) Frequency of FcR $\gamma$ <sup>-</sup> (left) and PLZF<sup>-</sup> (right) NK cells at the first malaria episode compared with their

frequency in May. Red dots indicate the 10 subjects with the highest relative increase between May and malaria episode. **(H)** Time to first malaria episode during the 2014 transmission season. The top 10 subjects listed in G are shown in red. P values determined with log rank Mantel–Cox test. **(I)** Frequency of FcR $\gamma$ <sup>-</sup> (left) and PLZF<sup>-</sup> (right) NK cells in December 2013 compared with their frequency in May, displayed as in G. **(J)** Time to first malaria episode during the 2014 transmission season, displayed as in H. P values determined with log rank Mantel–Cox test. Flow cytometry data in A, C–F, and I were acquired as in Fig. 1. Neg., negative.

frequency of FcR $\gamma$ <sup>-</sup> NK cells was significantly associated with age, showing a large transition at ~8 yr of age (Fig. 2 E). In contrast, the frequency of PLZF<sup>-</sup> NK cells had a wide distribution (~20% to ~80%) among young individuals, which gradually converged to a higher frequency with age (Fig. 2 E). A multiple linear regression model suggested a negative association of age with parasite load after adjustment for frequency of FcR $\gamma$ <sup>-</sup> NK cells ( $P = 0.035$ ) or PLZF<sup>-</sup> NK cells ( $P = 0.012$ ; Fig. S2 E). The frequency of PLZF<sup>-</sup> NK cells on its own, after adjustment for age, showed an inverse correlation with parasitemia ( $P = 0.044$ ; Fig. S2 E). Overall, these results suggest that adaptive FcR $\gamma$ <sup>-</sup> PLZF<sup>-</sup> NK cells contribute to protection against malaria.

#### Association of PLZF<sup>-</sup> NK cells with protection against future malaria episodes

Loss of PLZF expression is thought to be a precursor to epigenetic changes that turn off several genes, including the *FCER1G* gene for FcR $\gamma$  (Schlums et al., 2015; Tesi et al., 2016). Accordingly, Malian subjects had virtually no PLZF<sup>+</sup> FcR $\gamma$ <sup>-</sup> NK cells, and most subjects had a large proportion of FcR $\gamma$ <sup>+</sup> cells in the PLZF<sup>-</sup> subset (Fig. 2 F). Therefore, individuals with a high proportion of PLZF<sup>-</sup> FcR $\gamma$ <sup>+</sup> NK cells may be poised to increase the size of their PLZF<sup>-</sup> FcR $\gamma$ <sup>-</sup> cell subset.

Having shown that the frequency of FcR $\gamma$ <sup>-</sup> NK cells in May, before the transmission season, was significantly associated with resistance to malaria symptoms later, during the transmission season, we then asked whether an increase in FcR $\gamma$ <sup>-</sup> or PLZF<sup>-</sup> NK cell frequency in susceptible subjects during the transmission season would predict protection during malaria season in the following year (2014). The 10 subjects with the largest relative increase in FcR $\gamma$ <sup>-</sup> or PLZF<sup>-</sup> NK cell frequency between May 2013 and the first clinical malaria episode (Fig. 2 G) did not fare significantly better in 2014 (Fig. 2 H). However, the 10 subjects with the largest increase in PLZF<sup>-</sup> NK cells, but not FcR $\gamma$ <sup>-</sup> NK cells, between May and December 2013 (Fig. 2 I) had a significantly greater probability of remaining disease-free during the following year (Fig. 2 J). This would represent an age-independent contribution of PLZF<sup>-</sup> NK cells to protection, since within-subject changes in NK subset frequencies were used to assess differences in resistance to malaria during the subsequent year. It also supports the hypothesis that PLZF<sup>-</sup> FcR $\gamma$ <sup>+</sup> NK cells are the critical pool from which FcR $\gamma$ <sup>-</sup> NK cells arise.

#### Antibody-dependent NK cell responses are largely confined to FcR $\gamma$ <sup>-</sup> NK cells

The functionality of NK cells from all subjects was tested for their innate response to the HLA class I-negative tumor cell line 721.221 and for their activation by CD16 in an ADCC assay. To compare the contribution of different NK cell phenotypic

subsets to functional responses, we performed a t-SNE analysis of the overlay of all phenotypic markers included in functional assays (Fig. 3 A). Next, a computational analysis was performed to determine the probability NK cells in different phenotypic subsets had to produce IFN- $\gamma$  or degranulate in response to activation during natural cytotoxicity or ADCC (Fig. 3 B).

A large fraction of NK cells responded in the natural cytotoxicity assay, with multiple subsets having a good probability to produce IFN- $\gamma$  and to degranulate (Fig. 3, A and B). Notably, the presence or absence of FcR $\gamma$  in NK cells had little impact on the overall probability for response to 721.221 cells (Fig. 3, A and B). More specialized subsets were CD57<sup>-</sup> NKG2C<sup>-</sup> NKG2A<sup>+</sup> FcR $\gamma$ <sup>+</sup> NK cells for degranulation, and CD57<sup>+</sup> NKG2C<sup>+</sup> NKG2A<sup>-</sup> FcR $\gamma$ <sup>+</sup> NK cells for IFN- $\gamma$  (Fig. 3, A and B). IFN- $\gamma$  expressing CD56<sup>bri</sup> NK cells were also enriched in the NKG2C<sup>+</sup> subset (Fig. 3, A–C). As expected, CD56<sup>bri</sup> NK cells, which do not express CD16, did not respond in the ADCC assay (Fig. 3, A and B).

In marked contrast with the broad distribution of NK cells stimulated during natural cytotoxicity, functional responses in the ADCC assay were largely confined to the FcR $\gamma$ <sup>-</sup> NK cell subset (Fig. 3, A, B, and D). Conventional FcR $\gamma$ <sup>+</sup> NK cells responded poorly in the ADCC assay, despite good functionality in the natural cytotoxicity assay, suggesting that FcR $\gamma$ <sup>+</sup> NK cells have diminished ADCC responses during malaria. Enhanced cytokine production by FcR $\gamma$ <sup>-</sup> NK cells stimulated by CD16 occurred in CMV-induced adaptive NK cells (Lee et al., 2015; Schlums et al., 2015) and NK cells in HIV-infected individuals (Zhou et al., 2015). In our Mali cohort, NKG2A<sup>-</sup> FcR $\gamma$ <sup>-</sup> NK cells dominated both the IFN- $\gamma$  and the CD107a responses during ADCC (Fig. 3, A, B, and D). While CD57<sup>-</sup> NKG2C<sup>-</sup> NKG2A<sup>-</sup> FcR $\gamma$ <sup>-</sup> NK cells were more prone to degranulate (Fig. 3, A and B), CD57<sup>+</sup> NKG2C<sup>+</sup> NK cells were those enriched in the pool of IFN- $\gamma$ <sup>+</sup> NK cells, as observed also in the natural cytotoxicity assay (Fig. 3 E). A polyfunctional subset of NK cells, capable of responding during natural cytotoxicity and ADCC for IFN- $\gamma$  production and degranulation, was identified as NKG2C<sup>+</sup> NKG2A<sup>-</sup> FcR $\gamma$ <sup>-</sup> (Fig. 3, A and B). The basis for the enrichment of NKG2A<sup>-</sup> cells within responding cells triggered by CD16 (Fig. 3 D) is unclear. Perhaps licensing of NK cells through inhibitory killer-cell Ig-like receptors, which dominates in the absence of strong ligands for NKG2A (Horowitz et al., 2016), improves the ADCC response of NK cells from subjects in the Mali cohort. Genetic association studies on a larger cohort would be required to test this hypothesis.

As with every other phenotypic marker on CD56<sup>dim</sup> NK cells (Fig. 1 G), CD16 expression was bimodal, with a wide range of CD16<sup>+</sup> NK cell frequency among subjects (Fig. S3, A–C). CD16<sup>+</sup> NK cell frequency showed no correlation with susceptibility to malaria (Fig. S3 D). CD16<sup>-</sup> CD56<sup>dim</sup> cells can arise from activation-induced CD16 downmodulation (Jing et al., 2015).

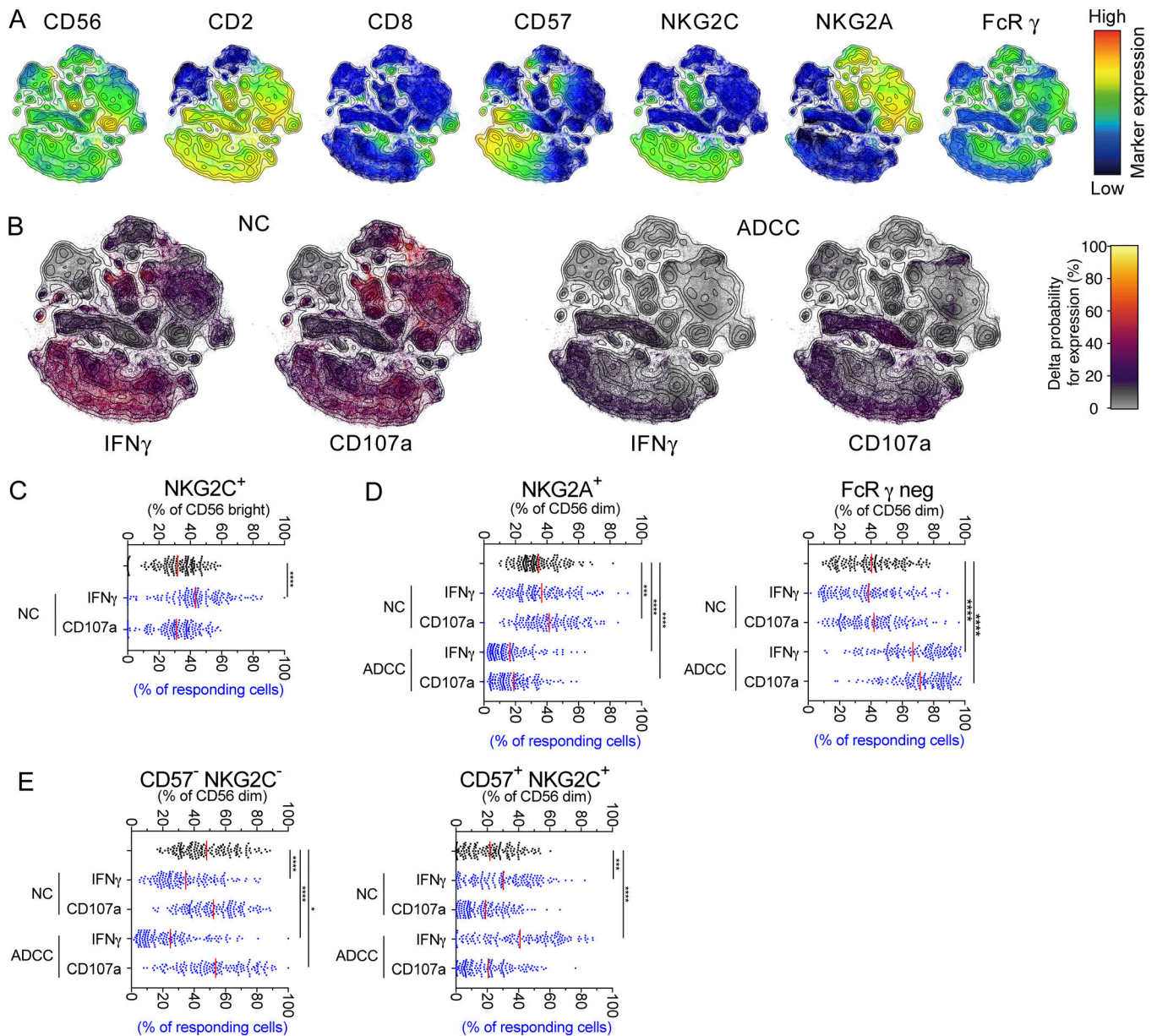


**Figure 3. Contribution of NK cell phenotypic subsets to functional responses.** **(A)** t-SNE analysis of NK cell phenotypic subsets in functional assays, combining controls (in the absence of target cells), natural cytotoxicity, and ADCC assays for all subjects at the May time point. A color scale indicates expression level. **(B)** Delta probability of IFN- $\gamma$  production and degranulation (CD107a) by NK cells stimulated in natural cytotoxicity (NC, left) and ADCC (right) assays. This probability, determined computationally and shown as a color scale, was overlaid on the same t-SNE distribution shown in A in order to identify specific phenotypic NK cell subsets that contributed to functional responses. The probability of a response in unstimulated controls was subtracted. **(C)** Frequency of NKG2C<sup>+</sup> NK cells among CD56<sup>bri</sup> NK cells for each subject (black dots), and among CD56<sup>bri</sup> NK cells that produced IFN- $\gamma$  or degranulated (CD107a) in the natural cytotoxicity assay (blue dots). One-way ANOVA with post hoc test comparing the responding cell frequency (blue) only to abundance (black). \*\*\*\*,  $P < 0.0001$ ; \*\*\*,  $P < 0.001$ ; \*,  $P < 0.05$ . **(D)** Analysis performed as in C for NKG2A<sup>+</sup> and FcR $\gamma$ <sup>-</sup> NK cells among CD56<sup>dim</sup> NK cells (black) and among CD56<sup>dim</sup> NK cells that responded in natural cytotoxicity and ADCC assays. **(E)** Analysis performed as in D for CD57<sup>-</sup> NKG2C<sup>-</sup> and CD57<sup>+</sup> NKG2C<sup>+</sup> NK cells. For C–E, one-way ANOVA with post hoc test comparing the responding cell frequency (blue) only to abundance (black). \*\*\*\*,  $P < 0.0001$ ; \*\*\*,  $P < 0.001$ ; \*,  $P < 0.05$ . Flow cytometry data in A and C–E were acquired as in Fig. 1.

Indeed, most NK cells that were activated to degranulate and to produce IFN- $\gamma$  were CD16<sup>-</sup> after stimulation (Fig. S3 E).

In chronic HIV-1 infection, the frequency of CD8<sup>+</sup> NK cells is associated with a delay in disease progression (Ahmad et al., 2014). In our Mali cohort, CD8<sup>+</sup> NK cell subsets showed no particular affiliation with other phenotypic markers or functional responses (Fig. 3, A and B).

The main conclusion from this functional analysis is that NK cell responses to Ab-coated target cells were largely confined to the FcR $\gamma$ <sup>-</sup> NK cell subset. Furthermore, phenotypic NK cell subsets with the most significant enrichment in resistant subjects were also the strongest responders to CD16-induced degranulation. Resistant subjects compared with subjects with a high parasite load, and susceptible subjects with the longest

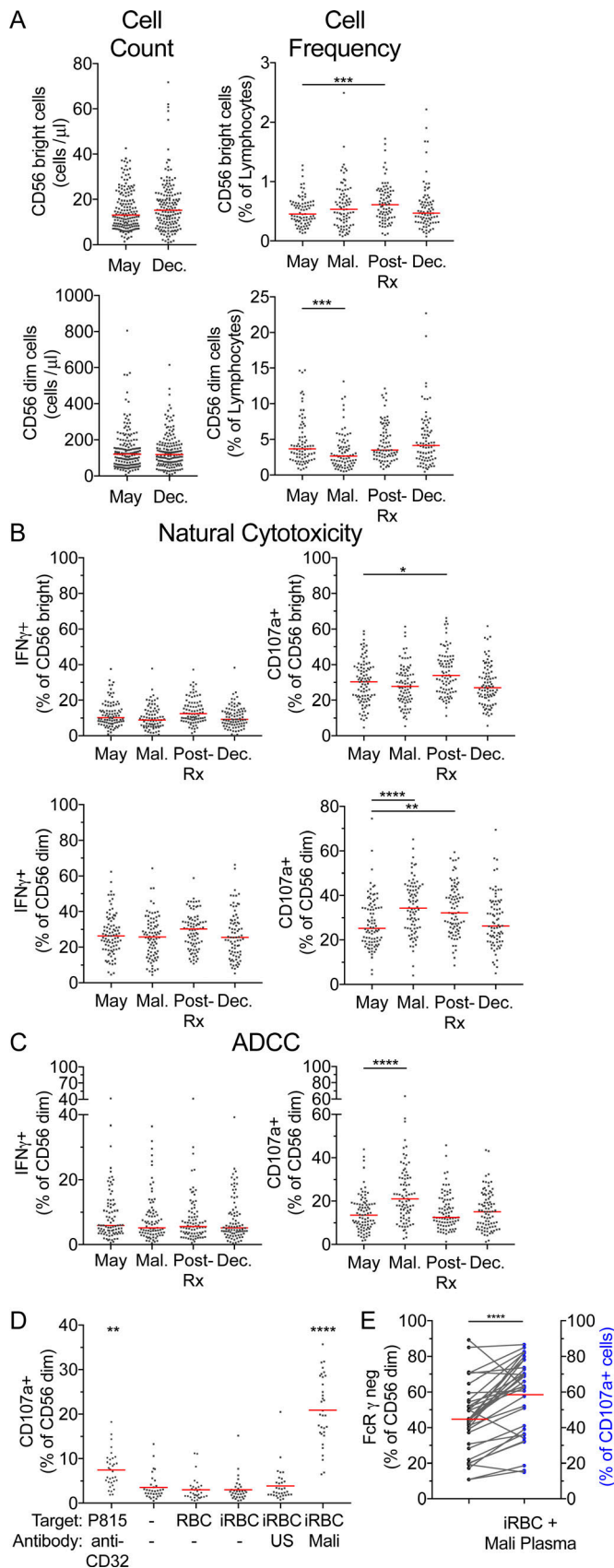


Figure 4. **Longitudinal analysis of NK cells during the malaria season and NK cell degranulation in response to *P. falciparum*-infected RBCs.** (A) CD56<sup>bri</sup> (top panels) and CD56<sup>dim</sup> (lower panels) NK cell number per

delay to first malaria episode, had significantly higher proportions of CD57<sup>-</sup> FcR $\gamma$ <sup>-</sup> NK cells (Fig. S2). The highest probability of degranulation in response to CD16 was in the NKG2A<sup>-</sup> FcR $\gamma$ <sup>-</sup> subset of NK cells (Fig. 3, A, B, and D). The strong degranulation potential of FcR $\gamma$ <sup>-</sup> NK cells in Mali subjects could result in lysis of infected RBCs through ADCC, thereby reducing parasitemia and contributing to clinical immunity to malaria.

### Elevated degranulation potential of CD56<sup>dim</sup> NK cells during malaria episodes

The number of NK cells per unit of blood did not vary significantly from before (May) to after (December) the malaria transmission season (Fig. 4 A). The proportion of CD56<sup>dim</sup> NK cells among lymphocytes decreased during episodes of febrile malaria, and recovered 7 d after anti-malaria treatment (Fig. 4 A). In contrast, the proportion of CD56<sup>bri</sup> NK cells among lymphocytes increased 7 d after treatment (Fig. 4 A). The opposite relative changes in CD56<sup>dim</sup> and CD56<sup>bri</sup> NK cell abundance suggest they were not caused by large fluctuations in total lymphocyte numbers. Such rapid changes could be due to NK cell adhesion in the vasculature or homing to peripheral tissue during acute infection. IFN- $\gamma$  responses stimulated by natural cytotoxicity and ADCC did not change longitudinally (Fig. 4, B and C). In contrast, a significantly higher proportion of CD56<sup>dim</sup> NK cells degranulated during acute malaria relative to pre-malaria season samples (Fig. 4, B and C). As resistance to malaria symptoms requires control of parasite load and of the associated inflammatory response, the selective increase in degranulation without increase in IFN- $\gamma$  production may contribute to protection by limiting inflammation. Anti-inflammatory responses required to reduce fever during malaria may include production of IL-10 by CD4 T cells (Portugal et al., 2017b) and by human NK cells stimulated with IL-15 (Burrack et al., 2018).

microliter at the May and December time points (left panels) and NK cell frequency among total lymphocytes (right panels) at the four time points in May, at the first malaria episode (Mal.), 7 d after treatment (Post-Rx), and in December (Dec.). For cell numbers, an unpaired *t* test was used. For cell frequency, one-way ANOVA with post hoc test was performed comparing malaria episode, Post-Rx, or December to the May time point only. \*\*\*, *P* < 0.001. (B) Functional responses of CD56<sup>bri</sup> (top panels) and CD56<sup>dim</sup> (lower panels) NK cells for IFN- $\gamma$  production (left panels) and degranulation (right panels) in the natural cytotoxicity assay. One-way ANOVA with post hoc test comparing malaria episode, Post-Rx, or December to the May time point. \*\*\*, *P* < 0.001; \*\*, *P* < 0.01; \*, *P* < 0.05. (C) Functional response of CD56<sup>dim</sup> NK cells in the ADCC assay across longitudinal time points. One-way ANOVA with post hoc test comparing malaria, Post-Rx, or December to the May time point only. \*\*\*\*, *P* < 0.0001. (D) PBMCs of 30 Malian subjects were tested for CD56<sup>dim</sup> NK cell degranulation in response to *P. falciparum*-infected RBC. The ADCC assay (P815 + anti-mouse CD32) used in Fig. 3 was performed here for comparison. PBMCs were incubated in the absence (-) or presence of RBC and of *P. falciparum*-infected RBC (iRBC), as indicated. Serum from US adults (US) and plasma from Mali adults were added, as indicated. One-way ANOVA was done with post hoc analysis comparing each group with the NK cell only control. \*\*\*\*, *P* < 0.0001; \*\*, *P* < 0.01. (E) FcR $\gamma$ <sup>-</sup> NK cell frequency among CD56<sup>dim</sup> NK cells (black symbols) and among CD107a<sup>+</sup> CD56<sup>dim</sup> NK cells stimulated by iRBC in the presence of Mali plasma (blue symbols). A paired *t* test was performed. \*\*\*\*, *P* < 0.0001. Flow cytometry data in A–C were acquired as in Fig. 1. Flow cytometry data in D and E were acquired over three independent experiments (*n* = 30).

### Activation of FcR $\gamma$ <sup>-</sup> NK cells by *P. falciparum*-infected RBCs and plasma of malaria-immune individuals

We tested the ability of NK cells in 30 PBMC samples from Malian subjects to respond to *P. falciparum*-infected RBCs. NK cell natural cytotoxicity degranulation in the presence of infected RBCs was no higher than basal degranulation observed in the presence or absence of uninfected RBCs (Fig. 4 D). In contrast, addition of plasma from malaria-resistant Mali adults, but not healthy US adults, to infected RBCs triggered ADCC degranulation by NK cells (Fig. 4 D). Notably, degranulation was considerably higher than that obtained in the generic ADCC assay used to screen samples from the larger cohort (Fig. 4 D). Furthermore, FcR $\gamma$ <sup>-</sup> cells were significantly enriched in the pool of degranulating NK cells (Fig. 4 E). As NK cells from US donors were capable of lysing *P. falciparum*-infected RBCs through an Fc receptor-dependent activation by IgG antibodies, and in the presence of the same Mali plasma sample used here (Arora et al., 2018), individuals in the Mali cohort, many of whom have a large proportion of FcR $\gamma$ <sup>-</sup> NK cells, are well equipped to eliminate infected RBCs through ADCC by NK cells. These results, and the high-frequency FcR $\gamma$ <sup>-</sup> NK cell association with disease resistance, demonstrated a strong potential of adaptive FcR $\gamma$ <sup>-</sup> NK cells to execute antibody-dependent control of malaria.

### Implications

Control of infectious disease through NK-mediated ADCC is an emerging theme, as a large study of *Mycobacterium tuberculosis*-infected individuals with active disease or latent tuberculosis showed that latency was consistently associated with increased NK cell abundance and enhanced cytotoxicity mediated by CD16 and NK cells (Roy Chowdhury et al., 2018). A direct test of the contribution of adaptive NK cells to protection from malaria through ADCC responses is not feasible in humans. However, the correlation of PLZF<sup>-</sup> FcR $\gamma$ <sup>-</sup> NK cell abundance among subjects in the cohort with reduced parasite load and reduced susceptibility to malaria symptoms warrants further investigations. Translation of our findings to clinical applications would include protocols to enhance the generation of adaptive NK cells, which are inherently strong responders to activation by CD16. In addition, vaccines that elicit IgG1 and IgG3 antibodies to *P. falciparum* antigens expressed at the surface of infected RBCs would provide high-affinity ligands for CD16. In vitro ADCC assays with NK cells are amenable to high-throughput screens of serum samples. In conclusion, our results suggest that NK cells play a critical and underappreciated role in reducing malaria morbidity through ADCC-mediated clearance of parasites from the blood.

## Materials and methods

### Human subjects

An ongoing prospective cohort study of naturally acquired malaria immunity in 695 children and adults was initiated in May 2011 in Kalifabougou, Mali, where intense, seasonal transmission of *P. falciparum* malaria occurs during the rainy season from June through December (Dumbo et al., 2014). During the dry season from January through May, there is little to no malaria

transmission (Portugal et al., 2017b). At least two cross-sectional collections were conducted during each year of the cohort study: one at the premalaria season baseline (May) and the second at the end of the malaria season (December). At each cross-sectional visit, a complete medical history and physical examination were performed along with blood collection by venipuncture and finger stick. Subjects are followed by active malaria surveillance consisting of scheduled clinic visits with finger stick blood collection for malaria diagnosis and passive surveillance consisting of symptom-triggered self-referred visits. Blood smears were performed for malaria diagnosis on any subject with malaria symptoms. Subjects with any detectable parasitemia were treated for malaria according to the National Malaria Control Program guidelines in Mali, which recommend artemether-lumefantrine for uncomplicated *P. falciparum* malaria. For this study, malaria susceptibility was defined as at least one malaria episode (temperature >37.5°C and *P. falciparum* parasitemia >2,500 parasites/ $\mu$ l) during a single malaria season, while malaria resistance was defined as no malaria episode during the same surveillance period. We used venipuncture blood samples from 2013 at the premalaria season baseline (May), during the first febrile malaria episode, 7 d after treatment (convalescence), and at the end of the malaria season (December). In Mali, blood was collected by venipuncture into sodium citrate-containing cell preparation tubes (Vacutainer CPT; Becton Dickinson). Plasma and PBMCs were separated according to the manufacturer's instructions. Plasma was frozen at -80°C. PBMCs were frozen in fetal bovine serum (GIBCO BRL) containing 7.5% DMSO (Sigma-Aldrich), kept at -80°C for 24 h, and then stored at -196°C in liquid nitrogen. Samples from Mali were shipped on dry ice (-78.5°C) over a course of 3 d using a courier service to Rockville, MD, where PBMC and plasma samples were again stored in liquid nitrogen vapor phase and at -80°C, respectively. Dried blood spots were used to determine the *P. falciparum* parasite load using real-time PCR amplification of *P. falciparum* genes as previously described (Tran et al., 2013).

### Sample selection for flow cytometric analysis

From an initial cohort of 695 subjects, we selected PBMCs from 200 subjects based on age, *P. falciparum* PCR-negative status at the May 2013 time point, malaria susceptibility, and sample availability. To reduce batch effects, the order of the subjects in the Mali cohort for sample analysis for phenotype and function was randomized, but longitudinal samples from each subject were analyzed at the same time. After analysis, samples that did not meet quality control (e.g., poor antibody staining of internal reference samples, low cell viability) were removed, resulting in a final analysis of samples from 163 subjects (Fig. 1 A and Fig. S1 A).

### Phenotype and functional assays

In a single day, 24–48 PBMC samples including three quality control PBMC samples described below were thawed. Batches of six PBMC samples (~5 million cells per tube) were thawed rapidly in a 37°C water bath into 15-ml conical tubes. 1 ml of prewarmed Roswell Park Memorial Institute-1640 media supplemented with 10% fetal bovine serum (RP10) was added, and the



tubes were swirled by hand. This step was repeated twice. Then the 15-ml conical tubes were filled with RP10 and centrifuged at  $650 \times g$ . Media was aspirated, and the cell pellets were re-suspended in 4.5 ml of RP10 supplemented with 10  $\mu\text{g}/\text{ml}$  gentamycin, and 5 U/ml DNase (Roche). Cells were then “rested” overnight in a 6-well plate. After 16 h, cells were removed from the plates and filtered (70  $\mu\text{m}$ ) into 5-ml FACS tubes. All cells, including 721.221 and P815 cell lines, were then counted on a FACS machine (LSR II) using counting beads (Invitrogen) and propidium iodide (Sigma-Aldrich) to assess numbers of living cells. One million PBMCs were used to stain phenotypic markers. Two samples of half a million PBMCs were mixed separately with 100,000 721.221 cells or 125,000 P815 cells. The mouse mastocytoma cell line P815 was first incubated with 2.5  $\mu\text{g}/\text{ml}$  anti-mouse CD32 (clone 2.4G2; Bio-X-Cell). Brefeldin A (Sigma-Aldrich) was added to a 1  $\mu\text{g}/\text{ml}$  final concentration, Monensin (Sigma-Aldrich) to 2  $\mu\text{M}$  final, and anti-CD107a (BioLegend) at 1:200 to the samples, and cells were incubated for 5 h at 37°C in 5%  $\text{CO}_2$ .

For the phenotype panel, approximately one million PBMCs were assessed. The primary surface stain was done in PBS for 20 min at room temperature in the dark. Information on antibodies used is found in Fig. S3 F. The secondary stain with live/dead stain was also done in PBS for 20 min at room temperature in the dark. Next, cells were washed and then incubated in 2% methanol-free electron microscopy-grade formaldehyde in PBS at 37°C for 10 min. After fixation, the cells were washed and centrifuged at  $750 \times g$  for 3 min and supernatants were discarded, and the same washing/centrifugation was done after each remaining step. Cells were permeabilized with 0.04% Triton for 7 min at room temperature. Anti-Eat-2 (rabbit IgG) antibody was then incubated with cells in PBS with 2% FBS, 2 mM EDTA, and 2% BSA (internal FACS buffer) for 20 min at room temperature. Cells were then stained with goat anti-rabbit polyclonal antibody in internal FACS buffer for 20 min at room temperature in the dark. The final internal stains were with anti-PLZF, anti-FcR $\gamma$  (Fc $\epsilon$ RI $\gamma$ ), and anti-Syk in internal FACS buffer with an additional 10% rabbit serum, to block any residual anti-rabbit Ig staining, for 2 h at room temperature in the dark. For the functional panel, cells were stained in the same way except for the following differences. The fixation with formaldehyde was done at room temperature. The final stain for FcR $\gamma$  chain and IFN- $\gamma$  was done for 30 min instead of 2 h. The samples were analyzed on a LSR II cytometer with a violet (405 nm), blue (488 nm), green (562 nm), and red (632 nm) laser set up.

Quality control of staining was accomplished by including the same three PBMC samples in every batch analyzed for phenotype and function. For each malaria-resistant subject in the cohort, there were two samples, collected in May and in December. For each of the malaria-susceptible subjects in the cohort, there were four samples, collected in May, at the malaria episode, 7 d after treatment, and in December. Samples from 18 Swedish subjects that had been analyzed previously in Sweden (Schlums et al., 2015) were included in this study to evaluate reproducibility. The data generated in this study correlated highly with previous staining results.

## Flow analysis

Statistical analysis of flow data was performed using FlowJo (TreeStar). For the Boolean analysis of phenotype data, positive gates for CD2, CD57, NKG2C, NKG2A, PLZF, and FcR $\gamma$  were determined and all single, double, and triple combinations (232 combinations) of those six markers were entered, and the frequency of resulting populations was tabulated for each subject. The markers CD8, Eat-2, and Syk were not included in the Boolean analysis due to the low proportion of CD8 $^+$ , Eat-2 $^-$ , and Syk $^-$  NK cells. For the analysis of functional data, the markers PLZF, Eat-2, and Syk were replaced with markers for cytokine production and degranulation.

## Distribution of NK cell functional responses among NK cell phenotypic subsets

For stochastic neighbor embedding analyses (van der Maaten and Hinton, 2008), preprocessing was performed as elsewhere (Schlums et al., 2015), and the R package Rtsne (<https://github.com/jkrijthe/Rtsne>) was used. To visualize how the NK cell CD107a and IFN- $\gamma$  responses were distributed over the phenotypic subsets, the single-cell  $\Delta$  response probability was calculated using the formula

$$\Delta P(\text{response})_x = \mu NN_{xStim} - \mu NN_{xCtrl},$$

where  $x$  denotes an individual cell,  $\mu NN_{xStim}$  and  $\mu NN_{xControl}$  denote the average positivity (CD107a or IFN- $\gamma$ ) among  $x$  and the 99 nearest neighbors to  $x$  in the stimulated sample that  $x$  was drawn from (ADCC or natural cytotoxicity), or among the 99 nearest neighbors to  $x$  in the unstimulated control, respectively. A cell was defined as positive if the following criterion was met:

$$FI_x > (\tilde{x}(FI_{Ctrl}) + 2MAD(FI_{Ctrl})),$$

where  $FI_x$  denotes the fluorescence intensity (CD107a or IFN- $\gamma$ ) of  $x$ ,  $\tilde{x}$  and  $MAD$  denote the median and the median absolute deviation, respectively, and  $FI_{Ctrl}$  is the fluorescence intensity in the unstimulated control sample from the same individual (patient or control) that  $x$  was drawn from. With this criterion, 6.5 and 2.5% of all the cells in the unstimulated control were defined as positive for CD107a and IFN- $\gamma$ , respectively. The 99 nearest neighbors were identified with the k-nearest neighbor algorithm (Cover and Hart, 1967) in the seven-dimensional space defined by CD2, CD8, CD56, CD57, FcR $\gamma$ , NKG2A, and NKG2C, including all unstimulated cells or cells from the ADCC or the natural cytotoxicity condition, respectively. For this analysis, the k-nearest neighbor algorithm implementation in the R package FNN was used (Beygelzimer et al., 2018). After this calculation, the delta response probability variables for CD107a and IFN- $\gamma$  were displayed on a t-SNE field generated with CD2, CD8, CD56, CD57, FcR $\gamma$ , NKG2A, and NKG2C as input dimensions.

## Activation of NK cells by *P. falciparum*-infected RBCs

RBCs infected with *P. falciparum* 3D7 strain and enriched for trophozoite stage were used to assess natural cytotoxicity and ADCC responses in cultures with PBMC. ADCC was tested with infected RBCs and a pool of plasma from malaria-immune Mali adults (Arora et al., 2018). Plasma from healthy, malaria-unexposed US donors was used as control. The ratio of PBMC to RBC target

was 1:1, totaling 1 million cells per well. Brefeldin A, monensin, and mAb to CD107a were added as described in the assay with P815 cells, and samples were incubated for 5 h at 37°C in RPI0 in 5% CO<sub>2</sub>.

### Testing for CMV and EBV

The presence of IgG for EBV and CMV antigens in plasma samples was analyzed using Liaison assays on a DiaSorin Liaison XL analyzer according to the manufacturer's instructions. Qualitative determination of specific IgG to human CMV antigens, and EBV antigens EBNA1 or VCA, was by indirect chemiluminescence immunoassay. Of the two EBV antigens tested, EBNA1 is expressed during latency, and VCA is typically expressed during the lytic cycle (Taylor et al., 2015). The main components of the test were magnetic particles coated with the viral proteins of interest and a conjugate of mAb to human IgG linked to an isoluminol derivative. During a first incubation, antibodies added to calibrators, samples, or controls bound to the magnetic particles. During a second incubation, the antibody conjugate reacted with viral specific IgG that was already bound to the magnetic particle. After each incubation, unbound material was removed with a wash cycle. Subsequently, the starter reagents were added, and a flash chemiluminescence reaction was induced. The light signal, and subsequent amount of isoluminol-antibody conjugate, was measured by a photomultiplier as relative light units and was indicative of the presence of viral specific IgG antibodies present in calibrators, samples or controls. Approximately 140 μl of plasma was used from each subject. Positive signals were determined using the manufacturer's recommendations of relative light units.

### Statistical analysis

Statistical analysis was performed using Prism 7 (Graphpad software), Excel version 16.14.1 (Microsoft), and R version 3.4.4. As noted in the figures, one-way ANOVA analysis was done for most graphs where means were shown and post hoc P value multiple comparison tests were determined using Sidak's test. For Kaplan–Meier analysis, the P values given were from a log rank Mantel–Cox test. Linear and nonlinear regression analysis and R<sup>2</sup> goodness-of-fit calculations were performed with Prism. The P value of the correlation of the two variables was determined using Pearson correlation analysis in Prism. To determine the relationship between specific NK subsets and parasite density, multiple linear regression was performed using log (parasites per microliter) as the dependent variable and the age (in years) and NK subset frequency (either FcRγ<sup>-</sup> or PLZF<sup>-</sup> NK cells in separate models) as independent covariates.

### Ethics statement

The Ethics Committee of the Faculty of Medicine, Pharmacy, and Dentistry at the University of Sciences, Techniques, and Technologies of Bamako, and the Institutional Review Board (IRB) of the National Institute of Allergy and Infectious Diseases, National Institutes of Health (NIH), approved this study (National Institute of Allergy and Infectious Diseases IRB-approved protocols 07-I-N141 and 06-I-N147). Written informed consent was obtained from all participants before inclusion in this study. Written informed consent and consent to publish was obtained from parents or

guardians of participating children before inclusion in the study. Peripheral blood samples from healthy US adults were obtained from the NIH Department of Transfusion Medicine under an NIH IRB-approved protocol (99-CC-0168) with informed consent.

### Online supplemental material

Fig. S1 provides information on subjects who participated in the study; a comparison of NK phenotypic subsets between Malian and Swedish subjects; serological data on EBV and CMV, and their correlation with NK phenotypic markers; and Boolean distribution of NKG2C, CD57, and FcRγ markers on NK cells in Malian subjects. Fig. S2 lists NK cell subsets most enriched in resistant subjects; and shows the relationship of parasite load with age, and a multiple linear regression analysis of the association of age, FcRγ<sup>-</sup> NK, and PLZF<sup>-</sup> NK cells with parasite load. Fig. S3 shows flow cytometry analysis of CD16 expression on NK cells from the study participants and its relationship to malaria resistance, and of CD16 expression after stimulation of NK cells; and provides detailed information on antibodies used in phenotypic and functional experiments.

### Acknowledgments

We thank Takele Yazew for technical help and the residents of Kalifabougou, Mali, for their participation in this study.

The study was funded by the Division of Intramural Research, National Institute of Allergy and Infectious Diseases, National Institutes of Health, AI000525-30 LIG (E.O. Long) and AI001155-06 LIG (P.D. Crompton).

The authors declare no competing financial interests.

Author contributions: conceptualization: G.T. Hart, P.D. Crompton, Y.T. Bryceson, and E.O. Long; methodology: G.T. Hart, T.M. Tran, J. Theorell, H. Schlums, S. Rajagopalan, P.D. Crompton, Y.T. Bryceson, and E.O. Long; investigation: G.T. Hart, G. Arora, A.D.J. Sangala, and K.J. Welsh; formal analysis: G.T. Hart, T.M. Tran, and J. Theorell; resources: B. Traore, S.K. Pierce, and P.D. Crompton; writing—original draft: G.T. Hart and E.O. Long; writing—review and editing: G.T. Hart, T.M. Tran, J. Theorell, H. Schlums, S. Rajagopalan, S.K. Pierce, P.D. Crompton, Y.T. Bryceson, and E.O. Long; supervision: Y.T. Bryceson and E.O. Long; and funding acquisition: S.K. Pierce, P.D. Crompton, Y.T. Bryceson, and E.O. Long.

Submitted: 31 August 2018

Revised: 19 January 2019

Accepted: 22 March 2019

### References

- Ahmad, F., H.S. Hong, M. Jäckel, A. Jablonka, I.N. Lu, N. Bhatnagar, J.M. Eberhard, B.A. Bollmann, M. Ballmaier, M. Zielinska-Skowronek, et al. 2014. High frequencies of polyfunctional CD8<sup>+</sup> NK cells in chronic HIV-1 infection are associated with slower disease progression. *J. Virol.* 88: 12397–12408. <https://doi.org/10.1128/JVI.01420-14>
- Arora, G., G.T. Hart, J. Manzella-Lapeira, J.Y. Doritchamou, D.L. Narum, L.M. Thomas, J. Brzostowski, S. Rajagopalan, O.K. Doumbo, B. Traore, et al. 2018. NK cells inhibit *Plasmodium falciparum* growth in red blood cells via antibody-dependent cellular cytotoxicity. *eLife.* 7:e36806. <https://doi.org/10.7554/eLife.36806>

- Bates, M., and A.B. Brantsaeter. 2016. Human cytomegalovirus (CMV) in Africa: a neglected but important pathogen. *J. Virus Erad.* 2:136–142.
- Beygelzimer, A., S. Kakadet, J. Langford, S. Arya, D. Mount, and S. Li. 2018. *FNN: Fast Nearest Neighbor Search Algorithms and Applications*. <https://CRAN.R-project.org/package=FNN>.
- Boyle, M.J., L. Reiling, G. Feng, C. Langer, F.H. Osier, H. Aspelung-Jones, Y.S. Cheng, J. Stubbs, K.K. Tetteh, D.J. Conway, et al. 2015. Human antibodies fix complement to inhibit *Plasmodium falciparum* invasion of erythrocytes and are associated with protection against malaria. *Immunity*. 42:580–590. <https://doi.org/10.1016/j.immuni.2015.02.012>
- Brodin, P., V. Jovic, T. Gao, S. Bhattacharya, C.J. Angel, D. Furman, S. Shen-Orr, C.L. Dekker, G.E. Swan, A.J. Butte, et al. 2015. Variation in the human immune system is largely driven by non-heritable influences. *Cell*. 160:37–47. <https://doi.org/10.1016/j.cell.2014.12.020>
- Burrack, K.S., M.A. Huggins, E. Taras, P. Dougherty, C.M. Henzler, R. Yang, S. Alter, E.K. Jeng, H.C. Wong, M. Felices, et al. 2018. Interleukin-15 Complex Treatment Protects Mice from Cerebral Malaria by Inducing Interleukin-10-Producing Natural Killer Cells. *Immunity*. 48:760–772.e4. <https://doi.org/10.1016/j.immuni.2018.03.012>
- Bustamante, L.Y., G.T. Powell, Y.C. Lin, M.D. Macklin, N. Cross, A. Kemp, P. Cawkill, T. Sanderson, C. Crosnier, N. Muller-Sienherth, et al. 2017. Synergistic malaria vaccine combinations identified by systematic antigen screening. *Proc. Natl. Acad. Sci. USA*. 114:12045–12050. <https://doi.org/10.1073/pnas.1702944114>
- Cohen, S., I.A. McGREGOR, and S. Carrington. 1961. Gamma-globulin and acquired immunity to human malaria. *Nature*. 192:733–737. <https://doi.org/10.1038/192733a0>
- Cover, T., and P. Hart. 1967. Nearest neighbor pattern classification. *IEEE Trans. Inf. Theory*. 13:21–27. <https://doi.org/10.1109/TIT.1967.1053964>
- Crompton, P.D., J. Moebius, S. Portugal, M. Waisberg, G. Hart, L.S. Garver, L.H. Miller, C. Barillas-Mury, and S.K. Pierce. 2014. Malaria immunity in man and mosquito: insights into unsolved mysteries of a deadly infectious disease. *Annu. Rev. Immunol.* 32:157–187. <https://doi.org/10.1146/annurev-immunol-032713-102220>
- Doumbo, S., T.M. Tran, J. Sangala, S. Li, D. Doumtable, Y. Kone, A. Traoré, A. Bathily, N. Sogoba, M.E. Coulibaly, et al. 2014. Co-infection of long-term carriers of *Plasmodium falciparum* with *Schistosoma haematobium* enhances protection from febrile malaria: a prospective cohort study in Mali. *PLoS Negl. Trop. Dis.* 8:e3154. <https://doi.org/10.1371/journal.pntd.0003154>
- Foley, B., S. Cooley, M.R. Verneris, M. Pitt, J. Curtsinger, X. Luo, S. Lopez-Vergès, L.L. Lanier, D. Weisdorf, and J.S. Miller. 2012. Cytomegalovirus reactivation after allogeneic transplantation promotes a lasting increase in educated NKG2C<sup>+</sup> natural killer cells with potent function. *Blood*. 119:2665–2674. <https://doi.org/10.1182/blood-2011-10-386995>
- Hammer, Q., T. Rückert, E.M. Borst, J. Dunst, A. Haubner, P. Durek, F. Heinrich, G. Gasparoni, M. Babic, A. Tomic, et al. 2018. Peptide-specific recognition of human cytomegalovirus strains controls adaptive natural killer cells. *Nat. Immunol.* 19:453–463. <https://doi.org/10.1038/s41590-018-0082-6>
- Holmes, T.D., and Y.T. Bryceson. 2016. Natural killer cell memory in context. *Semin. Immunol.* 28:368–376. <https://doi.org/10.1016/j.smim.2016.05.008>
- Horowitz, A., Z. Djaoud, N. Nemat-Gorgani, J. Blokhuis, H.G. Hilton, V. Beziat, K.J. Malmberg, P.J. Norman, L.A. Guethlein, and P. Parham. 2016. Class I HLA haplotypes form two schools that educate NK cells in different ways. *Sci. Immunol.* 1:eaag1672.
- Jing, Y., Z. Ni, J. Wu, L. Higgins, T.W. Markowski, D.S. Kaufman, and B. Walcheck. 2015. Identification of an ADAM17 cleavage region in human CD16 (FcγRIII) and the engineering of a non-cleavable version of the receptor in NK cells. *PLoS One*. 10:e0121788. <https://doi.org/10.1371/journal.pone.0121788>
- Khusmith, S., and P. Druilhe. 1983. Antibody-dependent ingestion of *P. falciparum* merozoites by human blood monocytes. *Parasite Immunol.* 5:357–368. <https://doi.org/10.1111/j.1365-3024.1983.tb00751.x>
- Lee, J., T. Zhang, I. Hwang, A. Kim, L. Nitschke, M. Kim, J.M. Scott, Y. Kamimura, L.L. Lanier, and S. Kim. 2015. Epigenetic modification and antibody-dependent expansion of memory-like NK cells in human cytomegalovirus-infected individuals. *Immunity*. 42:431–442. <https://doi.org/10.1016/j.immuni.2015.02.013>
- Lopez-Vergès, S., J.M. Milush, B.S. Schwartz, M.J. Pando, J. Jarjoura, V.A. York, J.P. Houchins, S. Miller, S.M. Kang, P.J. Norris, et al. 2011. Expansion of a unique CD57<sup>+</sup>NKG2Chi natural killer cell subset during acute human cytomegalovirus infection. *Proc. Natl. Acad. Sci. USA*. 108:14725–14732. <https://doi.org/10.1073/pnas.1110900108>
- Manicklal, S., V.C. Emery, T. Lazzarotto, S.B. Boppana, and R.K. Gupta. 2013. The “silent” global burden of congenital cytomegalovirus. *Clin. Microbiol. Rev.* 26:86–102. <https://doi.org/10.1128/CMR.00062-12>
- Portugal, S., N. Obeng-Adjei, S. Moir, P.D. Crompton, and S.K. Pierce. 2017a. Atypical memory B cells in human chronic infectious diseases: An interim report. *Cell. Immunol.* 321:18–25. <https://doi.org/10.1016/j.cellimm.2017.07.003>
- Portugal, S., T.M. Tran, A. Ongoiba, A. Bathily, S. Li, S. Doumbo, J. Skinner, D. Doumtable, Y. Kone, J. Sangala, et al. 2017b. Treatment of Chronic Asymptomatic *Plasmodium falciparum* Infection Does Not Increase the Risk of Clinical Malaria Upon Reinfection. *Clin. Infect. Dis.* 64:645–653. <https://doi.org/10.1093/cid/ciw849>
- Rotman, H.L., T.M. Daly, R. Clynes, and C.A. Long. 1998. Fc receptors are not required for antibody-mediated protection against lethal malaria challenge in a mouse model. *J. Immunol.* 161:1908–1912.
- Roy Chowdhury, R., F. Vallania, Q. Yang, C.J. Lopez Angel, F. Darboe, A. Penn-Nicholson, V. Rozot, E. Nemes, S.T. Malherbe, K. Ronacher, et al. 2018. A multi-cohort study of the immune factors associated with *M. tuberculosis* infection outcomes. *Nature*. 560:644–648. <https://doi.org/10.1038/s41586-018-0439-x>
- Schlums, H., F. Cichocki, B. Tesi, J. Theorell, V. Beziat, T.D. Holmes, H. Han, S.C. Chiang, B. Foley, K. Mattsson, et al. 2015. Cytomegalovirus infection drives adaptive epigenetic diversification of NK cells with altered signaling and effector function. *Immunity*. 42:443–456. <https://doi.org/10.1016/j.immuni.2015.02.008>
- Sun, J.C., J.N. Beilke, and L.L. Lanier. 2009. Adaptive immune features of natural killer cells. *Nature*. 457:557–561. <https://doi.org/10.1038/nature07665>
- Taylor, G.S., H.M. Long, J.M. Brooks, A.B. Rickinson, and A.D. Hislop. 2015. The immunology of Epstein-Barr virus-induced disease. *Annu. Rev. Immunol.* 33:787–821. <https://doi.org/10.1146/annurev-immunol-032414-112326>
- Tesi, B., H. Schlums, F. Cichocki, and Y.T. Bryceson. 2016. Epigenetic Regulation of Adaptive NK Cell Diversification. *Trends Immunol.* 37:451–461. <https://doi.org/10.1016/j.it.2016.04.006>
- Tran, T.M., S. Li, S. Doumbo, D. Doumtable, C.Y. Huang, S. Dia, A. Bathily, J. Sangala, Y. Kone, A. Traore, et al. 2013. An intensive longitudinal cohort study of Malian children and adults reveals no evidence of acquired immunity to *Plasmodium falciparum* infection. *Clin. Infect. Dis.* 57:40–47. <https://doi.org/10.1093/cid/cit174>
- van der Maaten, L., and G. Hinton. 2008. Visualizing Data using t-SNE. *J. Mach. Learn. Res.* 9:2579–2605.
- Wolf, A.S., S. Sherratt, and E.M. Riley. 2017. NK Cells: Uncertain Allies against Malaria. *Front. Immunol.* 8:212. <https://doi.org/10.3389/fimmu.2017.00212>
- Zhou, J., F.S. Amran, M. Kramski, T.A. Angelovich, J. Elliott, A.C. Hearps, P. Price, and A. Jaworowski. 2015. An NK Cell Population Lacking FcγR Is Expanded in Chronically Infected HIV Patients. *J. Immunol.* 194:4688–4697. <https://doi.org/10.4049/jimmunol.1402448>